UNIVERSIDAD NACIONAL DE COLOMBIA
SEDE MEDELLÍN
FACULTAD DE MINAS

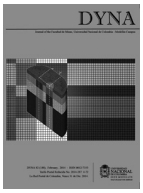

DYNA
http://dyna.medellin.unal.edu.co/

Elastoplastic behavior of longitudinally stiffened girder webs subjected to patch loading and bending

Carlos Graciano [a], Euro Casanova [b] & David G. Zapata-Medina [c]

[a] Facultad de Minas, Universidad Nacional de Colombia, Medellín, Colombia. cagracianog@unal.edu.co
[b] División de Ciencias Físicas y Matemáticas, Universidad Simón Bolívar, Caracas, Venezuela. ecasanov@usb.ve
[a] Facultad de Minas, Universidad Nacional de Colombia, Medellín, Colombia. dgzapata@unal.edu.co

Received: February 20th, 2014. Received in revised form: September 8th, 2014. Accepted: September 16th, 2014.

Abstract
This paper is aimed at studying the elastoplastic behavior of longitudinally stiffened girder webs subjected to patch loading and bending. The investigation is carried out by means of nonlinear finite element analysis to study the structural behavior of the girder components (flanges, web and stiffener) at ultimate limit state. Initial geometrical imperfections, plastic material behavior and large deflection effects are considered in the model. For the numerical model validation, the computer results from the simulations are compared with experimental results taken from the literature. A parametric study was carried out in order to investigate the influence of the applied bending moment and the relative location of the stiffener on the ultimate strength to patch loading.

Keywords: girders; structural stability; nonlinear finite elements; patch loading; bending; longitudinal stiffeners.

Comportamiento elastoplástico de vigas rigidizadas longitudinalmente sometidas a carga concentrada y momento flector

Resumen
Este artículo está enfocado en estudiar el comportamiento elastoplástico de vigas rigidizadas longitudinalmente en el alma y sujetas a combinaciones de carga concentrada y momento flector. La investigación se realiza mediante un análisis de elementos finitos no lineal para estudiar el comportamiento estructural de los diferentes componentes de la viga (aletas, alma y rigidizador) bajo el estado límite de carga. El modelo considera los efectos de imperfecciones geométricas iniciales, comportamiento plástico del material y grandes deflexiones. La validación del modelo numérico se hace mediante comparación directa de los resultados numéricos con valores experimentales disponibles en la literatura técnica. Finalmente, se realiza un estudio paramétrico con el objeto de investigar la influencia del momento flector y la localización del rigidizador en la resistencia última de la viga bajo cargas concentradas.

Palabras clave: vigas; estabilidad estructural; elementos finitos no lineales; carga concentrada; momento flector; rigidizadores longitudinales.

1. Introduction

In current practice, longitudinal stiffeners are primarily introduced in bridge girder webs in order to increase the resistance to shear and/or bending. For these two load types, the influence of longitudinal stiffeners has been extensively investigated and included in design codes. In order to account for the interaction between patch loading and bending moments, the formulae available for unstiffened webs are often used for longitudinally stiffened girder webs.

Regarding the behavior of longitudinally stiffened girder webs subjected to combined patch loading and bending only a small number of tests results is available [1-4]. [1] showed an increase of 34% in the resistance of stiffened webs with respect to unstiffened girders. [3] demonstrated that by using closed section stiffener the increase in ultimate strength can be of 40%. Similar results were observed by [4]. Regarding the use of multiple stiffeners, [2, 4 and 5] showed that the use of two stiffeners placed close to the loaded flange leads to an increase in patch loading resistance.

Finite element simulations have also been used to gain more knowledge in this field [4, 6-11]. In particular, the

experiments performed recently by [4] were aimed at investigating the influence of the patch loading length. The results from that investigation showed that current formulae used for longitudinally stiffened girders underestimate the patch loading resistance when the patch load length is large. In a similar manner, [9] investigated by mean of finite element analysis the influence of girder depth and patch load length. Once again, the results showed an underestimation of the patch loading resistance when using the current formulae available in the literature [12].

A large amount of the research previously mentioned herein has been aimed at studying the influence of the following parameters: 1) presence of global bending (ratio between the applied bending moment and the bending resistance M/M_R); 2) presence of a longitudinal stiffener (unstiffened versus stiffened); 3) position of a longitudinal stiffener (b_1/h_w); and 4) number of longitudinal stiffeners. The main conclusion of the aforementioned research works is that the presence of global bending reduces the ultimate strength of the webs under patch loading.

As evaluated by Graciano and Casanova [8], general recommendations to estimate the reduction in patch loading resistance due to the presence of global bending for longitudinally stiffened girders have been presented in terms of interaction equations. However, the reasons that lead to this reduction are not well understood. It may be explained by studying the elastoplastic behavior of the girder components by means of three variables: 1) the nonlinear load-displacement response, 2) an interaction surface response, and 3) the plastic strain distribution. In this paper, the girder components are modelled accounting for elastoplastic material behavior and geometrical nonlinearities, such as large displacement and initial shape imperfections. The results obtained from the FEM simulations are validated against results from full-scale laboratory experiments. Subsequently, a parametric study was conducted in order to investigate the influence of the relative position of the stiffener and the magnitude of the applied bending moment on the ultimate resistance to patch loading.

2. Nonlinear finite element model

The nonlinear computations were performed using the finite element program ANSYS [13]. Shell elements S181 from the ANSYS element library were used to model the web, flanges (top and bottom) and the longitudinal stiffener.

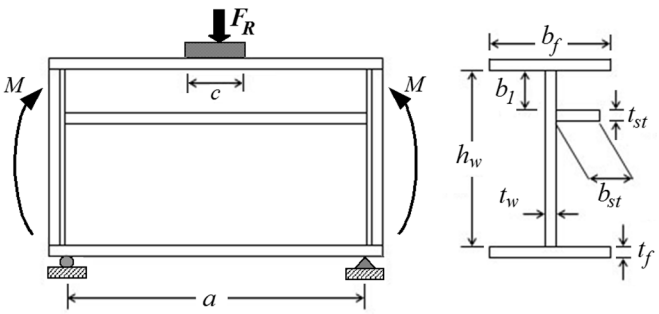

Figure 1. Stiffened plate girder under patch loading and bending.
Source: The authors.

This element accounts for finite strain and is suitable for large strain analysis as well as for complex buckling behavior. For the validation and corresponding parametric analysis, two girders, namely VT08 and VT10, tested experimentally [3] were used in the numerical analysis. Fig. 1 show the nomenclature used in the analysis, the sub-indexes *w* and *f* refer to web and flange, respectively.

For Girder VT08 the dimensions were: a =2480 mm; h_w = 1000 mm, t_f = 8.35 mm; b_f = 150 mm, c = 240 mm, b_1 = 200 mm; and the yield strengths for the web and flanges are f_{yw} = 358 MPa and f_{yf} = 328 MPa. For Girder VT10 the dimensions were basically the same, except for b_1 = 150 mm; and the material properties f_{yw} = 380 MPa and f_{yf} = 275 MPa. When modeling the plate materials (flange, web and stiffener), these were assumed to have a perfectly plastic behavior. The Young's modulus was set to 210 GPa and Poisson's ratio was set to 0.3.

Initially, the FEM model was performed considering only the patch loading case, thereafter, the combined action of patch loading and bending were considered. Due to the symmetry in the geometry, loads and boundary conditions, just one half of each plate girder was modelled as shown in Fig. 2.

Transverse stiffeners at the end of the plate girder were modelled by means of rigid body kinematic constraints of the degrees of freedom located in the corresponding side. [14] showed that this modeling assumption is only valid for small loading lengths (i.e., c/a < 0.25). The initial imperfections were introduced as sine waves in both the longitudinal and transverse directions, with a maximum amplitude w_o = 7 mm, in agreement with experimentally measured values reported by [3]. Out-of-plumbness geometric imperfections [15-16] have not been included in this analysis.

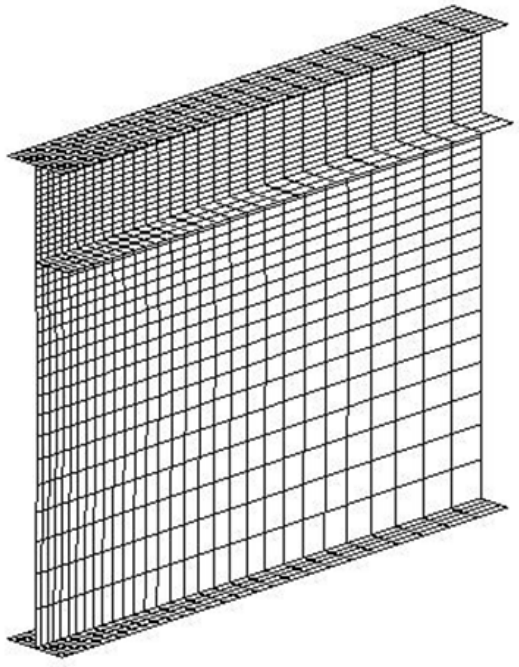

Figure 2. FEM model for girders VT08 and VT10.
Source: The authors.

Table 1.
Comparison of experimental and computed values using FEM for patch loading (F_R) and bending (M_R) resistances.

Girder	$F_{R\text{-}Exp}$ [kN]	$F_{R\text{-}FEM}$ [kN]	$M_{R\text{-}Exp}$ [kN.m]	$M_{R\text{-}FEM}$ [kN.m]
VT08-4	199	207	533	574
VT08-5/6	232	254	-	-
VT08-8	-	-	634	736
VT10-4	161	181	655	736
VT10-5/6	281	308	-	-

Source: The authors.

The patch load was transferred into the girder by loading all the nodes located in the web axis along the loading length $c/2$ with an equal value force. Displacement constraints were applied to the loaded nodes in the out-of-plane direction in function of a master node and all rotations were restrained. This master node was then displacement controlled in the FE analysis. The nonlinear path of the load-deflection curve was traced using the modified Riks method [17].

A convergence analysis was conducted using the ultimate resistance as parameter to calibrate the model, hence a mesh with 1620 elements was chosen (see Fig. 2). It is important to mention that the size of the elements was further reduced in the areas were the stress gradient was expected to changed. Table 1 shows a comparison between experimental and numerical results for girders VT08 and VT10. Moreover, it can be seen that the difference in patch loading and bending resistance from the FEM simulations is within 12 % of the experimentally measured values. It is worth quoting that the bending resistance in this paper is calculated using FEM simulations of the plate girder subjected to only bending.

3. Parametric analysis

In the previous section the FEM model was validated, and both the patch loading and bending resistances for girders VT08 and VT10 were computed numerically. In this section a parametric analysis is performed to study the influence on the nonlinear load-displacement response of the relative position of the stiffener (b_1/h_w), and the magnitude of the applied bending moment (M/M_R).

3.1. Influence of the stiffener position (b_1/h_w)

The relative location of the stiffener was varied from 0.05 h_w to 0.3 h_w for girders VT08 and VT10. For each location the magnitude of the applied bending moment was also varied. The nonlinear load-displacement responses of the girders are shown in Figs. 3 and 4.

Note that the maximum difference in the load-deflection curve of the girders for the various stiffener locations is reached at the ultimate load-state. Also, at the beginning of loading, the slope of the curves is quite similar. When the stiffener is placed at $b_1/h_w = 0.05$ (Figs. 3a and 4a) the curves are almost flat in the post-peak range for all the girders.

For the remaining stiffener locations ($0.10 \leq b_1/h_w \leq 0.30$), once the ultimate strength is achieved, the curves seem to follow a very similar path, especially in the range $0.19 \leq M/M_R \leq 0.76$. After this point the drop in the descending branch becomes sharper. In addition, for the stiffeners placed in this range the drop in the load becomes sharper when the distance b_1 from the loaded flange increases. This is due to an increase in the sensitivity toward the initial imperfections; *i.e.* the larger the subpanel formed between the loaded flange and the stiffener, the greater the influence of the amplitude of the initial imperfections.

In general, for values of bending moment of $M/M_R \geq 0.76$ the curves are very flat in the post-ultimate range (Figs. 3 and 4), this behavior is characteristic of plate girder webs subjected to predominant bending.

Table 2 gives a summary of the numerical results of the patch loading resistance (F_R) and bending resistance (M_R) for the various locations of the stiffener. For girders VT08 and VT10 the optimum position to increase the patch loading resistance is at $b_1/h_w = 0.10$. For these girders is important to notice that the ratio between the patch load length and the girder width (c/a) is equal to 0.1. A wider length makes the buckle under the loaded flange larger and consequently the crippling area also increases.

3.2 Magnitude of the applied bending moment (M/M_R)

The magnitude of the applied bending moment M was varied from 0.19 M_R to 0.9 M_R. Interaction curves for Girders VT08 and VT10 subjected to combined patch load and bending moment are shown in Fig. 5 for all the stiffener locations. After analyzing these two figures, the following conclusions can be drawn: a stiffener placed at $b_1/h_w = 0.20$ is better to improve the patch loading resistance in the presence of global bending in the range $M/M_R \leq 0.60$ approximately. This position corresponds also to the optimum of a longitudinal stiffener to increase the critical buckling load for girders subjected to bending [18]. For larger values of bending the best location is at $b_1/h_w = 0.05$. For this position, the stiffener is so close to the loaded flange that acts as a very stiff flange composed of the flange itself, the stiffener and the corresponding subpanel.

Table 2.
Patch loading (F_R) and bending (M_R) resistances for the girders.

Girder	b_1/h_w	F_R [kN]	M_R [kN.m]
VT08-4	0.05	243	707
	0.10	282	732
	0.15	268	753
	0.20	245	736
	0.25	232	729
	0.30	229	673
VT10-4	0.05	263	765
	0.10	295	805
	0.15	293	838
	0.20	267	836
	0.25	257	796
	0.30	252	775

Source: The authors

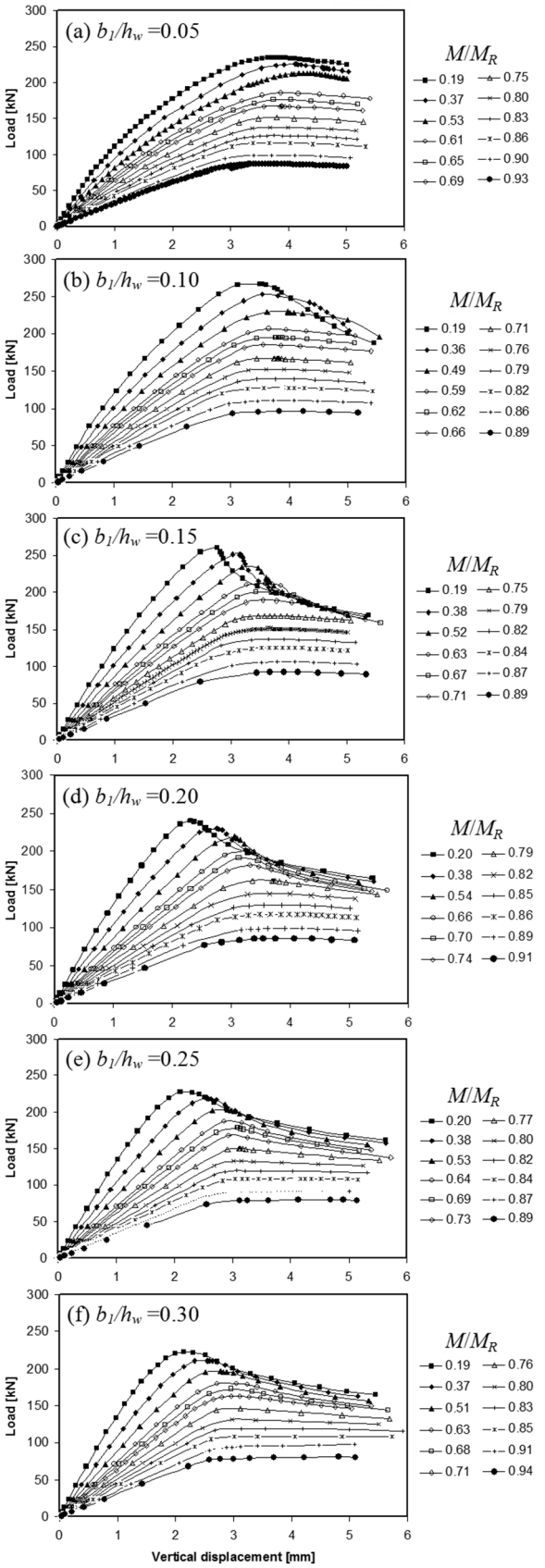

Figure 3. Load-deflection curves for girder VT08-4 for various stiffener locations (b_1/h_w).
Source: The authors.

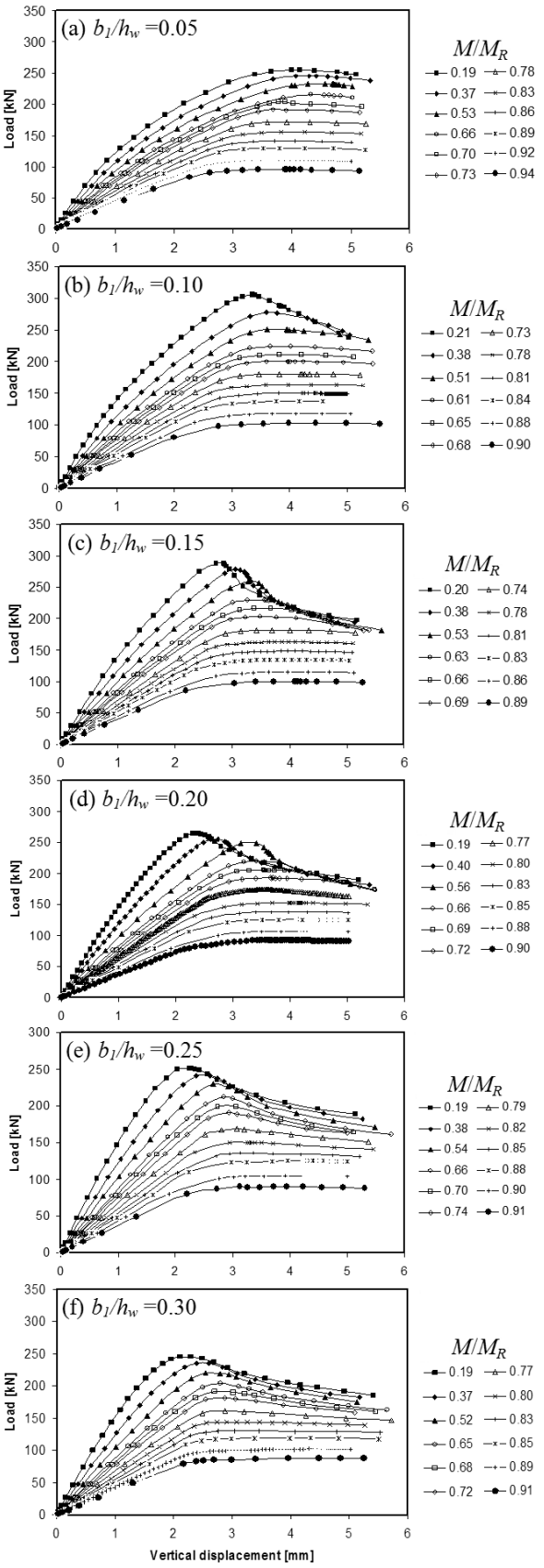

Figure 4. Load-deflection curves for girder VT10-4 for various stiffener locations (b_1/h_w).
Source: The authors.

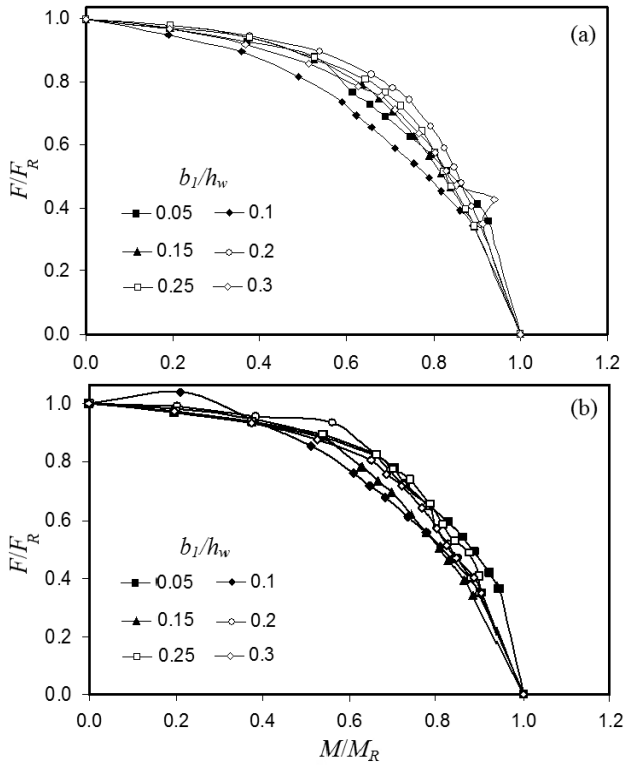

Figure 5. Interaction curves for (a) Girder VT08-4 and (b) Girder VT10-4.
Source: The authors

4. Numerical results

4.1. Structural behavior of the girder components

The structural behavior of the girder components can be better understood by analyzing the contour plots of stress distribution (von Mises and longitudinal stresses) and plastic strain distribution. The following figures show von Mises stress, longitudinal stress and plastic strain distributions for girders VT08 and VT10 used for the parametric analysis. These plots are calculated for two bending moments (M/M_R = 0.20 and M/M_R = 0.70).

Fig. 6 shows the longitudinal stress distribution for the flange and stiffener of girder VT08 at ultimate load state at two different levels of bending, 20% and 70% of the moment resistance M_R.(0.2M_R and 0.7M_R, respectively). As seen in this figure, the maximum compressive stress in the loaded flange increases of 18%, after increasing the magnitude of the applied bending moment. A greater increase is observed in minimum stress from 1.95 MPa to -75.56 MPa. Additionally, the stress distribution is more uniform for the larger bending moment. A similar situation is observed in Fig. 7 for the von Mises stress distribution.

In order to investigate the behavior of the web of girder VT08, Figs. 8 and 9 show the plots for longitudinal stress and von Mises stress distributions, respectively. In Fig. 8, once again the increase in the compressive stresses in the web beneath the patch load is very large (51%). When the bending moment increases the stress distribution becomes more uniform with respect to the neutral axis of the girder, which represents a typical feature of girder subjected to pure bending. In Fig. 9, the maximum stress occurs beneath the loaded flange for both cases of bending. The increase in longitudinal stresses due to bending is greater in the web than in the flange as observed in Figs. 6 and 8.

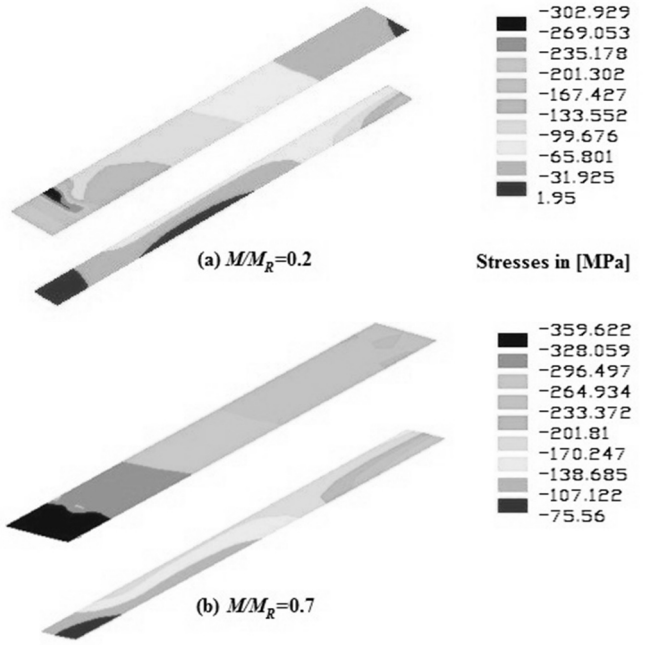

Figure 6. Plots for longitudinal stress distributions for Girder VT08 (flange and stiffener) at ultimate load level.
Source: The authors

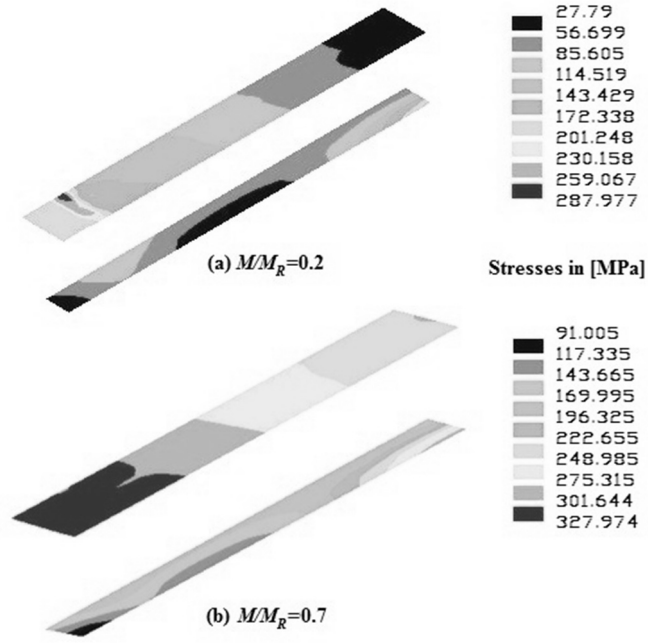

Figure 7. Plots for von Mises stresses for flange and stiffener of Girder VT08 at ultimate load level.
Source: The authors

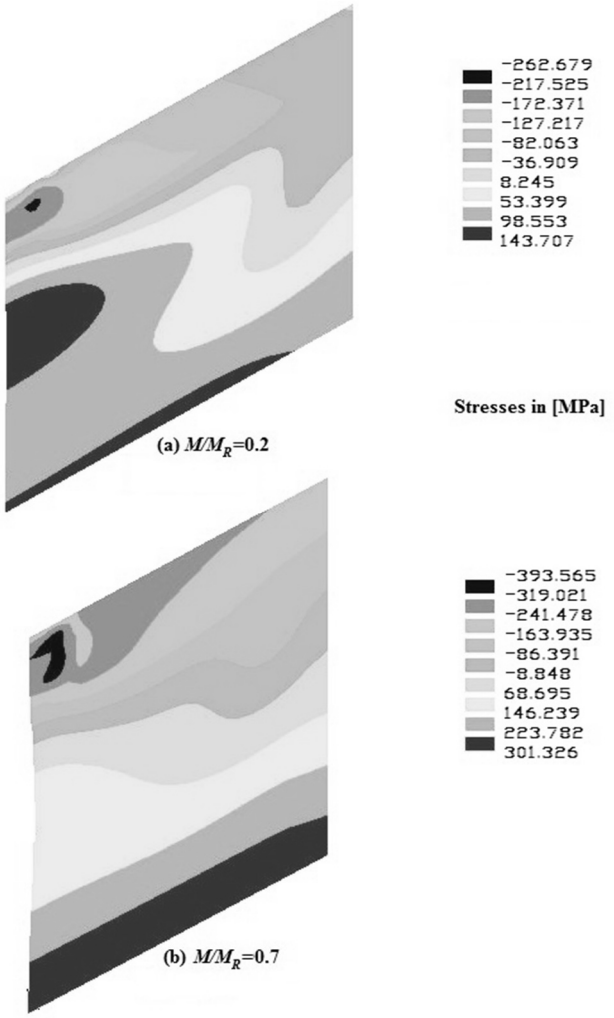

Figure 8. Plot for longitudinal stresses for the web of Girder VT08 at ultimate load level.
Source: The authors

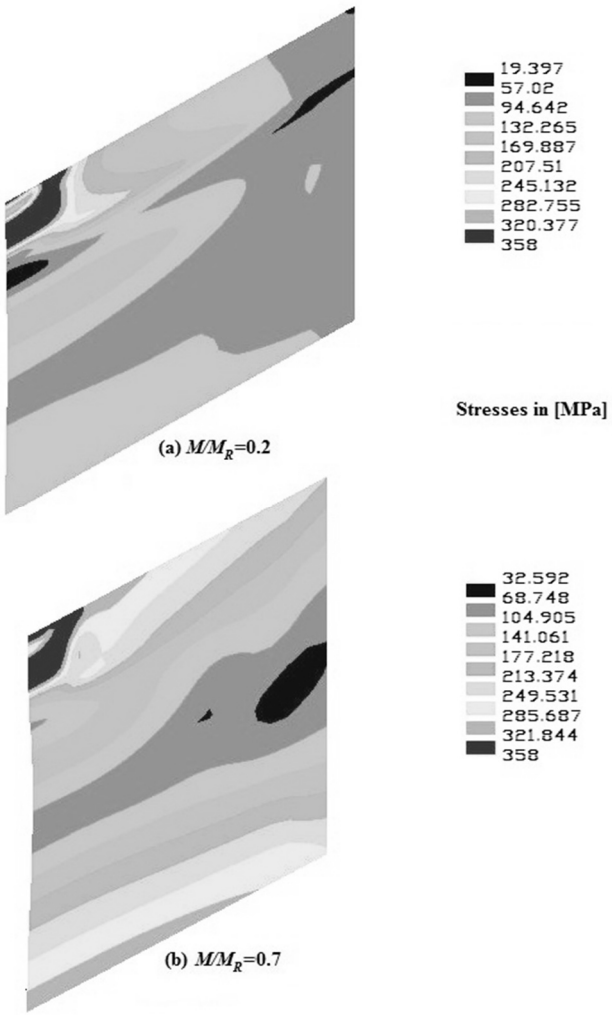

Figure 9. Plots of von Mises stresses for web of Girder VT08 at ultimate load level.
Source: The authors

Fig. 10 shows the plastic strain distribution for the full girder VT08. It is interesting to observe that for the lower bending moment a yield line appears only in the web (Fig. 10a). For the larger bending moment (Fig. 10b), the yield lines are fully developed in the web, and also plastic hinges can be observed in the compression flange.

A similar behavior was observed for girder VT10. However, the magnitude of the increase in longitudinal and von Mises stresses was smaller than for girder VT08. The flange of the former (t_f =12mm) is larger than for the latter (t_f =8mm). Consequently, girder VT10 is able to withstand effectively the stresses produced by bending.

Fig. 10 shows the plastic strain distribution for girder VT08 at ultimate load level. For small bending moments ($0.2M_R$), the yield lines appear only in the web plate (Fig. 10a) in the directly loaded subpanel. By increasing the applied bending moment ($0.7M_R$) the plate girder undergoes a larger plastic deformation, especially in the loaded flange, due mainly to the enhancement in longitudinal stresses over the compression flange. As seen in Fig. 10b, a plastic collapse mechanism is fully developed in the whole plate girder, i.e. presence of plastic hinges in the loaded flange and yield lines on the web.

5. Conclusions

The elastoplastic behavior of longitudinally stiffened girder webs under patch loading and bending was studied herein by means of the finite element method. The results show that an increase of the applied bending moment causes an increase in the magnitude of the longitudinal stresses in the girder components (loaded flange, web and even the stiffener). This increase in the longitudinal stresses leads to a reduction in the patch loading resistance. In the web the stress distribution becomes more uniform in the presence of bending.

It was demonstrated that, for large bending moments the best location to increase patch loading resistance of the stiffener is within b_1/h_w =0.20 and b_1/h_w =0.25, which also corresponds to the optimum position of a longitudinal stiffener to increase the critical buckling load.

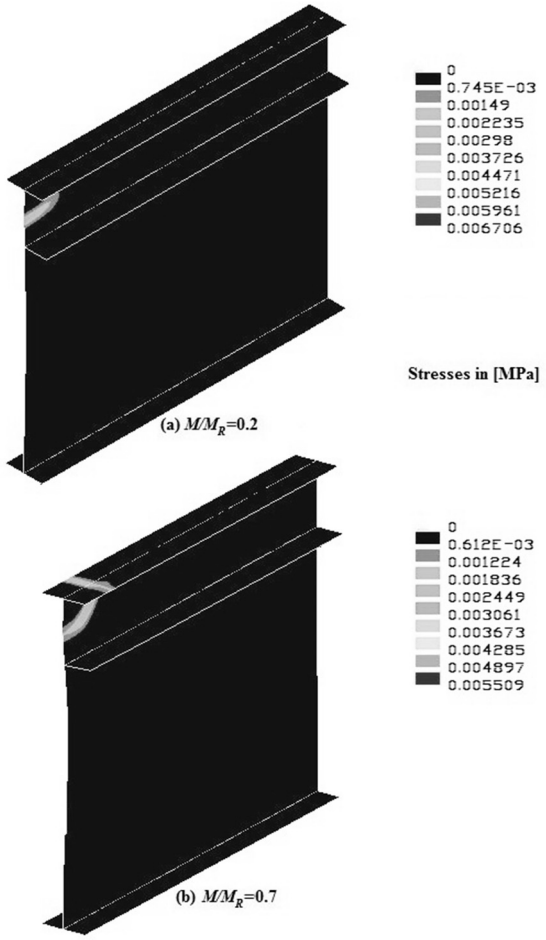

Figure 10. Plastic strain for Girder VT08 at ultimate load level.
Source: The authors

References

[1] Galea, Y., Godart, B., Radouant, I. and Raoul, J., Test of buckling of panels subject to in-plane patch loading, Proceedings of the ECCS Colloquium on Stability of Plate and Shell Structures, Ghent University, pp. 65-71, 1987.

[2] Shimizu, S. Belgium,, Yoshida, S. and Okuhara, H., An experimental study on patch loaded web plates, Proceedings of the ECCS Colloquium on Stability of Plate and Shell Structures, Ghent University, Belgium, pp. 85-94, 1987.

[3] Dubas, P. and Tschamper, H., Stabilité des âmes soumises à une charge concentrée et à une flexion globale. Construction Métallique, 2, pp. 25-39, 1990.

[4] Kuhlmann, U. and Seitz, M., Longitudinally stiffened girder webs subjected to patch loading, Proceedings of Steel Bridge - An International Symposium on Steel Bridges, Millau, France, 2004.

[5] Benedetti, A. and Dall'Aglio, F., Patch loading of longitudinally stiffened webs. Bridge maintenance, safety, management, resilience and sustainability: Proceedings of the Sixth International IABMAS Conference, Stresa, Lake Maggiore, Italy, pp. 1039-1046, 2012.

[6] Shimizu, S., The collapse behaviour of web plates on the launching shoe. Journal of Constructional Steel Research, 31 (1), pp. 59-72, 1994. http://dx.doi.org/10.1016/0143-974X(94)90023-X

[7] Dogaki, M., Nishijima, Y. and Yonezawa, H., Nonlinear behaviour of longitudinally stiffened webs in combined patch loading and bending, Proceedings of Constructional Steel Design, World Developments, pp. 141-150, 1992.

[8] Graciano, C. and Casanova, E., Ultimate strength of longitudinally stiffened I-girder webs subjected to combined patch loading and bending. *Journal of Constructional Steel Research*, vol. 61(1), pp. 93-111, 2005. http://dx.doi.org/10.1016/j.jcsr.2004.07.006

[9] Davaine, L., Raoul, J. and Aribert, J.M., Patch load resistance of longitudinally stiffened bridge girders, Proceedings of Steel Bridge - An International Symposium on Steel Bridges, Millau, France, 2004.

[10] Seitz, M., Tragverhalten langsversteifter Blechtrager unter quergerichteter Krafteinleitung, Ph.D. Thesis dissertation, Stuttgart University, Stuttgart, Germany, 2005.

[11] Braun, B. and Kuhlmann, U., The interaction behaviour of steel plates under transverse loading, bending moment and shear force, Proceedings of SDSS Rio 2010: International Colloquium Stability and Ductility of Steel Structures, Rio de Janeiro; Brazil, 2, pp. 731-738, 2010.

[12] Graciano, C., Strength of longitudinally stiffened webs subjected to concentrated loading. Journal of Structural Engineering, 131 (2), pp. 268-278, 2005. http://dx.doi.org/10.1061/(ASCE)0733-9445(2005)131:2(268)

[13] ANSYS, Inc. Elements Reference. Release 12.1. Canonsburg, USA. 2009. pp. 1688.

[14] Graciano, C., Mendez, J. and Zapata-Medina, D., Influence of the boundary conditions on FE-modeling of longitudinally stiff-ened I-girders subjected to concentrated loads. Rev. Fac. Ing. Univ. Antioquia, 71, pp. 221-229, 2014.

[15] Aristizabal-Ochoa, J., Induced moments and lateral deflections in columns with initial imperfections and semirigid connections: I. Theory. DYNA, 79 (172), pp. 7-17, 2012

[16] Aristizabal-Ochoa, J., Induced moments and lateral deflections in columns with initial imperfections and semirigid connections: II. Verification and examples. DYNA, vol. 79 (172), pp. 18-28, 2012

[17] Riks, E., An incremental approach to the solution of snapping and buckling problems. International Journal of Solids and Structures, vol. 15(7), pp. 529-551, 1979. http://dx.doi.org/10.1016/0020-7683(79)90081-7

[18] Rockey K.C. and Leggett, D.M.A., The buckling of a plate girder web under pure bending when reinforced by a single longitudinal stiffener. ICE Proceedings, 21 (1), pp. 161-188, 1962.

C. Graciano, received Bs. in 1992 and MSc. in 1995, both in Mechanical Engineering from the Simon Bolivar University, Venezuela. He later moved to Sweden where he obtained a Licentiate of Engineering in 2001 and a PhD. in 2002 in Structural Engineering from Chalmers University of Technology and Luleå University of Technology, Sweden, respectively. From 1997 to 2013, he served as Assistant, Associate and Full Professor in the Mechanical Engineering Department at the Simon Bolivar University, Venezuela. Currently, he is an Associate Professor in the Civil Engineering Department in the Facultad de Minas at the Universidad Nacional de Colombia, Medellin campus, Colombia. His research interests include: finite element modeling, structural stability, piping stress analysis and crashworthiness among others.

E. Casanova, received BS. in 1990 and MS. in 1996, both in Mechanical Engineering from the Simon Bolivar University, Venezuela. He later moved to France where he obtained a PhD in 2002 in Numerical modeling in Mechanical Engineering from Université de Technologie de Compiègne, France. Currently, he is an Associate Professor in the Mechanical Engineering Department at the Simon Bolivar University, Venezuela. His research interests include the study of the influence of uncertainties (i.e., material properties, geometry, boundary conditions, etc.) on the numerical modeling of different mechanical systems.

D.G. Zapata-Medina, received a BS. in 2004 in Civil Engineering from the Universidad Nacional de Colombia, Medellin campus, Colombia, a MSc. in 2007 in Geotechnical Engineering from the University of Kentucky, USA and a PhD. in 2012 in Geotechnics from Northwestern University, USA. Currently, he is an Assistant Professor in the Civil Engineering Department, in the Facultad de Minas at the Universidad Nacional de Colombia, Medellin campus, Colombia. His research interests include: soil characterization and constitutive soil modeling for geotechnical earthquake engineering applications; field instrumentation, numerical simulation and performance evaluation of earth retaining structures; and analytical and numerical solutions to calculate the static and dynamic stability of soil-structure interaction problems.